Statistical Short-Range Guidance for Peak Wind Forecasts on Kennedy Space Center/Cape Canaveral Air Force Station, Phase III

Winifred Crawford
Applied Meteorology Unit
Kennedy Space Center, Florida

May 2010

NASA STI Program ... in Profile

Since its founding, NASA has been dedicated to the advancement of aeronautics and space science. The NASA scientific and technical information (STI) program plays a key part in helping NASA maintain this important role.

The NASA STI program operates under the auspices of the Agency Chief Information Officer. It collects, organizes, provides for archiving, and disseminates NASA's STI. The NASA STI program provides access to the NASA Aeronautics and Space Database and its public interface, the NASA Technical Report Server, thus providing one of the largest collections of aeronautical and space science STI in the world. Results are published in both non-NASA channels and by NASA in the NASA STI Report Series, which includes the following report types:

- TECHNICAL PUBLICATION. Reports of completed research or a major significant phase of research that present the results of NASA Programs and include extensive data or theoretical analysis. Includes compilations of significant scientific and technical data and information deemed to be of continuing reference value. NASA counterpart of peer-reviewed formal professional papers but has less stringent limitations on manuscript length and extent of graphic presentations.

- TECHNICAL MEMORANDUM. Scientific and technical findings that are preliminary or of specialized interest, e.g., quick release reports, working papers, and bibliographies that contain minimal annotation. Does not contain extensive analysis.

- CONTRACTOR REPORT. Scientific and technical findings by NASA-sponsored contractors and grantees.

- CONFERENCE PUBLICATION. Collected papers from scientific and technical conferences, symposia, seminars, or other meetings sponsored or co-sponsored by NASA.

- SPECIAL PUBLICATION. Scientific, technical, or historical information from NASA programs, projects, and missions, often concerned with subjects having substantial public interest.

- TECHNICAL TRANSLATION. English-language translations of foreign scientific and technical material pertinent to NASA's mission.

Specialized services also include creating custom thesauri, building customized databases, and organizing and publishing research results.

For more information about the NASA STI program, see the following:

- Access the NASA STI program home page at *http://www.sti.nasa.gov*

- E-mail your question via the Internet to help@sti.nasa.gov

- Fax your question to the NASA STI Help Desk at (301) 621-0134

- Phone the NASA STI Help Desk at (301) 621-0390

- Write to:
  NASA STI Help Desk
  NASA Center for AeroSpace Information
  7121 Standard Drive
  Hanover, MD 21076-1320

Statistical Short-Range Guidance for Peak Wind Forecasts on Kennedy Space Center/Cape Canaveral Air Force Station, Phase III

Winifred Crawford
Applied Meteorology Unit
Kennedy Space Center, Florida

May 2010

Acknowledgements

Available from:

NASA Center for AeroSpace Information
7121 Standard Drive
Hanover, MD 21076-1320
(301) 621-0390

This report is also available in electronic form at

http://science.ksc.nasa.gov/amu/

Executive Summary

The peak winds are an important forecast element for the Expendable Launch Vehicle and Space Shuttle programs. The 45th Weather Squadron (45 WS) and the Spaceflight Meteorology Group (SMG), however, indicate that peak winds are a challenging parameter to forecast, particularly in the cool season. To alleviate some of the difficulty in making this forecast, the Applied Meteorology Unit (AMU) calculated cool season climatologies and distributions of 5-min mean and peak winds in Phase I. The 45 WS requested that the AMU update these statistics with more data collected since that time, use new time-period stratifications, and test another parametric distribution. These modifications will likely make the statistics more robust and useful to operations. The 45 WS also requested an Excel-based graphical user interface (GUI) similar to that from Phase II to display the mean and peak speed climatologies and probabilities. The AMU met all requests and delivered the GUI to the 45 WS for operational use.

The data used in this task were from the wind towers in the Kennedy Space Center (KSC)/Cape Canaveral Air Force Station (CCAFS) network used to evaluate weather launch commit criteria. The period of record increased from 7 cool seasons (October–April) in Phase I to 13 cool seasons (1995–2007) for this phase. The AMU used automated and manual data quality control methods on the data prior to analysis to ensure erroneous data had a minimal impact on the resulting statistics.

The AMU created the same climatologies and probabilities of mean and peak wind speeds similar to those in Phase I. The climatologies were created using the three stratifications of hour, direction, and direction/hour for each tower, height, and month. Diagnostic peak speed probabilities were created for each tower in each month for the 5-min mean speeds in 1-kt intervals. "Diagnostic" indicates that the peak speeds were observed in the same 5-min period as mean speed. Empirical, or observed, and parametric distributions fit to the empirical distributions were created. The parametric distribution was calculated to smooth over variations and fill gaps in empirical distributions, and extrapolate probabilities of peak speeds beyond the range of the observations. Tests revealed that the Gumbel distribution was a good fit to the data, except for some higher speeds. The AMU developed an objective two-step algorithm to determine the highest speed that could be modeled with the Gumbel distribution. More data due to a longer POR and this new objective cutoff method allowed higher speeds to be modeled in this phase than in Phase I.

The final set of statistics to be calculated were the prognostic probabilities that provide the climatological probability of meeting or exceeding a specified peak speed within a specified time period after a 5-min mean speed observation. The time periods requested by the 45 WS were 2, 4, 8, and 12 hours. The AMU developed a re-sampling technique to prepare the data that used all 5-min mean and peak speeds in the data set to calculate the observed probabilities. Results from several tests showed that no single parametric distribution could be used to model the prognostic probabilities. Therefore, only the observed prognostic probabilities were calculated.

The 45 WS also requested a PC-based GUI to display the probabilities and climatologies quickly and in an easy-to-interpret format. In Phase II, the AMU calculated the same statistics as in Phase I for the Shuttle Landing Facility towers to assist SMG in evaluating Flight Rules and a GUI to display the values. That GUI was modified to contain features needed by the 45 WS. The Phase III GUI is the result of several consultations between the AMU and 45 WS to ensure it met their needs, was easy to use, and produced useful information in a readable format.

Several factors create higher average wind speeds and influence the intensity of peak winds on KSC/CCAFS, including frontal passages, convective outflow boundaries, high momentum air mixed down from aloft, boundary layer stability, the distance between the tower and the ocean, and surface roughness surrounding the site (height, type, amount of vegetation). The peak speed distributions caused from any of these factors could result in different parametric distributions. The different phenomena that cause gusts could be mixed together, and each could create their own distribution that looks like a standard parametric distribution, but in reality is a mixture of distributions. The best way to determine the proper distributions would be to create data stratifications based on meteorological phenomena and other physical properties such as topography around the tower and stability.

It is important to remember that all climatology and probability values calculated in this task represent historical wind behavior. They are not predictive, and should not be used as an absolute forecast of future winds. They are intended to assist in making the forecast as an objective first guess. Model output, current observations, and forecaster experience should be used along with this tool to make a confident peak wind forecast.

Table of Contents

List of Figures

List of Tables

1. Introduction

The peak winds are an important forecast element for the Expendable Launch Vehicle and Space Shuttle programs. As defined in the Weather Launch Commit Criteria (LCC) and Shuttle Weather Flight Rules (FR), each vehicle has peak wind thresholds that cannot be exceeded in order to ensure safe launch and landing operations. The 45th Weather Squadron (45 WS) and the Spaceflight Meteorology Group (SMG) indicate that peak winds are a challenging parameter to forecast, particularly in the cool season months October – April. To alleviate some of the difficulty in making this forecast, the Applied Meteorology Unit (AMU) calculated cool season climatologies and probabilities of 5-min mean and peak winds in Phase I (Lambert 2002). The 45 WS requested the AMU update these statistics with more data collected since Phase I was completed, use new time-period stratifications, and test another parametric distribution. These modifications could make the statistics more robust and useful to operations. They also requested a graphical user interface (GUI) similar to that created in Phase II (Lambert 2003) to display the mean and peak speed climatologies and probabilities.

1.1 Operational Issues

As a vehicle launches, it could be forced into the tower by a strong wind gust. To avoid this, each launch operation has specific wind speed thresholds defined in the LCC that cannot be exceeded. The thresholds vary by vehicle, vehicle configuration, and wind direction. Launch vehicles are also exposed to the weather from the time their service tower is removed through launch, which could be up to 10 hours. If a launch is scrubbed, the vehicle is exposed for a longer period as it must be de-fueled before its service structure is put back in place. During this time period, the vehicle is susceptible to damage from winds that exceed a tolerance threshold. Such winds could cause airborne debris to impact and damage the vehicle, or cause the vehicle to oscillate to the point that it damages support lines or makes contact with its supporting structure. As a Shuttle lands, crosswinds that exceed the operational threshold could cause damage to the orbiter. The results of such damage would be costly, or possibly catastrophic with loss of human life.

Accurate forecasts of peak winds, therefore, are critical to protecting the safety of launch pad workers and astronauts as well as preventing financial losses due to delays and damage to the vehicle. Such forecasts are valuable to launch directors when deciding not only to launch but whether to continue with pre-launch procedures, and to flight directors who must decide whether to issue a GO for a Shuttle landing at the de-orbit burn decision time.

1.2 Previous AMU Work

In Phase I, the AMU created Microsoft® Excel® (hereafter Excel) Pivot Charts that displayed the hourly and directional climatologies for each tower used to evaluate the LCC and the probability of exceeding specific peak speed values given an observed or forecast mean wind speed value (Lambert 2002). The data were stratified by month prior to calculating the climatologies and probabilities. Two classes of probabilities were provided: empirical and parametric. The empirical, or observed, curves for the higher speeds became noisy due to smaller sample sizes. To alleviate this, the AMU fit a parametric distribution to the empirical distributions. This helped smooth the empirical distributions and estimate probabilities of peak speeds outside the range of the observations (Wilks 2006).

Phase II had two goals: 1) create the same statistics as in Phase I for the Shuttle Landing Facility towers used to evaluate shuttle FR, and 2) create a PC-based GUI to display the desired values quickly in an easily readable format (Lambert 2003). The Pivot Chart displays were very flexible and allowed the data to be viewed several different ways, but they proved difficult to manipulate and interpret during high-intensity operations. Therefore, the AMU created the GUI using Visual Basic for Applications (VBA) in Excel, which accessed the data in Pivot Tables.

1.3 Current Study

The goals of this task were to update the Phase I statistics for the LCC towers with an increased period of record (POR) from 7 to 13 years, use new time-period stratifications, test a different parametric distribution, and develop a GUI to display the statistics similar to the GUI created in Phase II. The main difference in this work from previous phases was the calculation of prognostic probabilities, i.e. the probability of meeting or exceeding a specified peak speed over the next few hours. The AMU accomplished all of these goals.

Section 2 of this report describes the data used in the calculations. Section 3 describes the creation of the statistics similar to those in Phase I, Section 4 describes the method used to calculate the prognostic probabilities, and Section 5 describes the GUI. A summary is provided in Section 6.

2.   Data

The data used in this task were from the wind towers in the Kennedy Space Center (KSC)/Cape Canaveral Air Force Station (CCAFS) network used to evaluate LCC. They were provided to the AMU by Computer Sciences Raytheon. The POR is the 13 cool seasons (October–April) in 1995–2007. Data before 1995 were not used due to a known noise problem in the archived peak winds that was fixed in late 1994 (William Roeder, 45 WS, personal communication). The analysis used only cool-season data since this was identified by the forecasters as being the most difficult time period in which to forecast peak winds. It is also a difficult forecast in the warm season, but the speeds are usually far below operational thresholds. If they exceed thresholds, it would likely be due to convection in the area. Other launch and safety criteria would be in effect if convection was close enough to cause high winds.

2.1   Wind Tower Data

The towers and heights used to evaluate the LCC are shown in Table 1. The locations of the pads and towers listed in Table 1 are shown in Figure 1.

Table 1.   Programs, towers, and sensor heights of data that were analyzed. (SLC=Space Launch Complex).

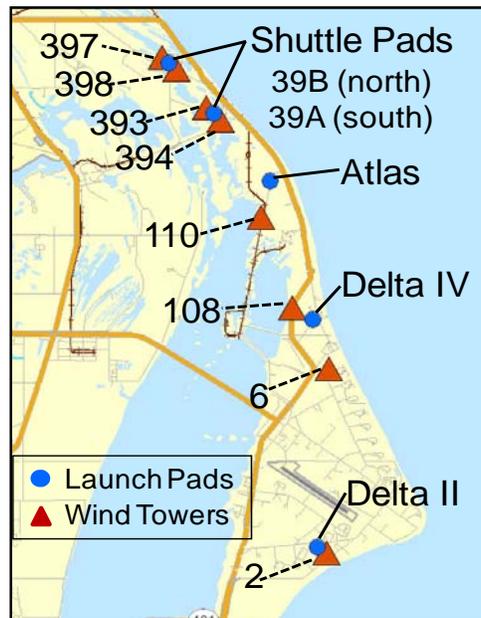| Launch Program	Tower(s)	Primary Height	Backup Height
Shuttle	393/394 (SLC 39A) 397/398 (SLC 39B)	60 ft	N/A
Atlas	110	204 ft	54 ft
Delta II	2	90 ft	54 ft
Delta IV	6, 108	54 ft	12 ft

Figure 1.   Map of the KSC/CCAFS area showing the locations of the wind towers described in Table 1.

9

Three of the towers in Table 1 have redundant sensors on opposing sides. Each side has its own number designation as shown in Table 2. Tower 108 has one sensor on the southeast side. The sensors at these towers were added in response to the effect of obstructed wind flow around the tower on the downwind sensor. They were also added so that one sensor could be used as a backup for the other in case of failure. Only data from the upwind side of each tower are displayed to the forecasters, but data from both sensors at each tower are collected and archived. The AMU processed and analyzed the data from both sensors at the redundant towers as separate sensors.

Table 2. Towers with redundant sensors and the location of the sensors relative to the towers. Each side of the tower is given a distinct number.

Tower Number	Side: Number
2	Northwest: 0020 Southeast: 0021
6	Northwest: 0061 Southeast: 0062
110	Northwest: 1101 Southeast: 1102

The data set contained the year/month/day/hour/minute/height of each observation with a time resolution of 5 minutes. The meteorological variables in the data set included

- Temperature and dew point temperature in Celsius,
- 5-min mean and peak wind speeds in ms^{-1},
- 5-min mean and peak wind direction in degrees,
- Deviation of the 5-min mean wind direction in degrees, and
- Relative humidity in percent.

The raw wind speed and direction data were sampled every second. The 5-min mean is the average of 600 1-second observations in a 5-min period. The peak is the maximum 1-second speed in the 5-min period. Before processing, the wind speeds were converted to knots (kt) with the conversion factor

$$kt = 1.9424 * ms^{-1}.$$

2.2 Quality Control

The AMU used automated and manual data quality control (QC) methods on the data prior to analysis to ensure erroneous data had a minimal impact on the resulting statistics.

2.2.1 Automated QC

The same automated QC algorithms described in Lambert (2002) were used here, with one exception: the peak-to-mean speed ratio check was replaced with a new equation. While conducting a task for SMG, Dr. Lee Burns at Marshall Space Flight Center (MSFC) identified errors in this check, which used the following logic, where MSPD = 5-min mean speed and R = maximum allowable ratio:

- MSPD < 2 kt, $R = \infty$
- MSPD = 2 kt, R = 10
- $3 \text{ kt} \leq MSPD \leq 8 \text{ kt}$, R = 2.6 + 0.16*MSPD
- MSPD > 8 kt, R = 2.5 below 50 ft, 2.0 above 50 ft

The MSPD was multiplied by R to get the maximum allowable peak speed. Any values above that threshold were flagged as erroneous. The blue curve in Figure 2 shows the resulting maximum peak speeds allowed for each 5-min mean speed using the logic above. The ratio value for 2 kt allowed a peak speed of 20 kt, but the equation for speeds 3–8 kt reduced the maximum peak speeds to 10–21 kt, respectively. This was not physically realistic. The maximum allowable peak speeds should increase with mean speed, not decrease from infinity at 0–1 kt mean speed to 20 kt at 2 kt mean speed, then to 10 kt at 3 kt mean speed.

The AMU fit a linear regression equation to the blue curve in Figure 2, and made adjustments to the slope and intercept to ensure realistic and internally consistent peak speed thresholds for each mean speed. The red curve in Figure 2 shows the maximum allowable peak speeds according to the equation

$$Peak = 2.2*MSPD + 10.6.$$

The discontinuity and inconsistencies at ≤ 8 kt mean speed from the previous algorithm (blue) were eliminated with the new algorithm (red), which shows a smooth and continuous increase in peak speed thresholds from low to high mean speedsThe AMU replaced the original algorithm described previously with the new linear regression equation in the QC program, and ran the program for all towers and heights in Table 1. A manual comparison between the original and new algorithms revealed that many valid peak speeds flagged by the original algorithm were not flagged by the new one, yet the new algorithm flagged more erroneous values.
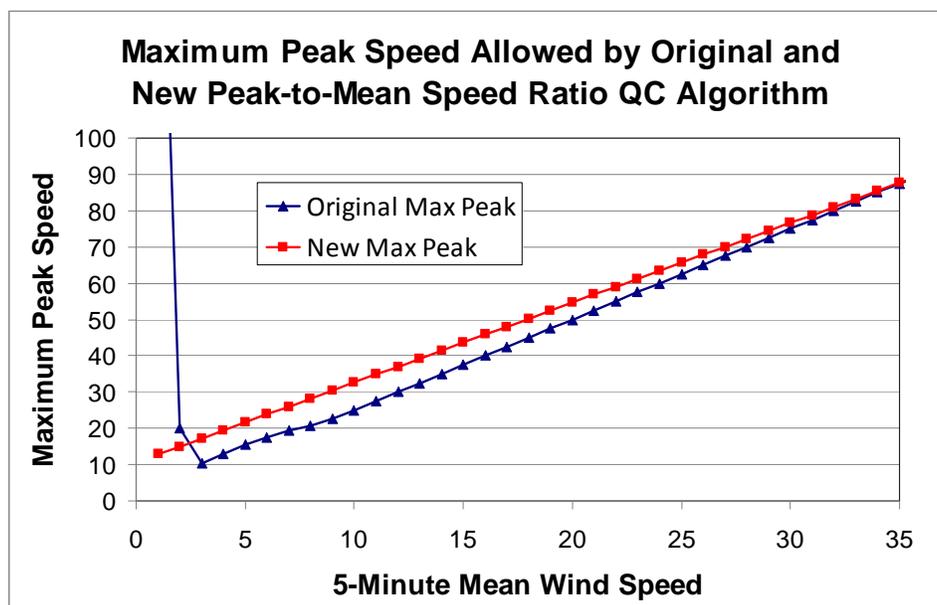
Figure 2. The curves showing the maximum allowable peak speed based on the 5-min mean speed (both in knots) using the original (blue) and the new (red) algorithms.

2.2.2 Manual QC

After running the automated QC program, the AMU noted time periods in which all of the observed values did not change. A manual check revealed the values to be erroneous when there were four or more in succession. The values were usually consistent with observations previous to the repetition but inconsistent with the values following the repetition. The cause of the unchanging values is unknown, but was likely a problem that occurred with the instrument, the data transmission, or the data recording. The AMU developed a script to find four or more repeated mean and peak speed and direction values, and then flagged them as erroneous. This check should be added to future automated QC of CCAFS/KSC tower winds.

As part of a task with Dr. Merceret (AMU Chief), the AMU found four October days during the POR in which the towers were affected by tropical storm winds: Josephine (1996), Irene (1999), Leslie (2000), and Wilma (2005). The goal of this task is to calculate statistics for cool season winds caused by cool-season phenomena, not tropical storm winds. These data would contaminate the climatology and probability values and were flagged as erroneous and removed from the subsequent analysis.

11

2.3   Stratification

After QC, the data were stratified by month and sensor (tower/height/side). For the climatologies discussed in Section 3.1, the data were further stratified by hour and direction. For the probabilities discussed in Sections 3.2 and 4, the data were stratified by mean speed in 1-kt increments. The hourly and directional stratifications are described in more detail in Section 3.1.

It is important to note that the AMU did not stratify the data by stability prior to calculating the climatologies and probabilities. The 45 WS tasked the AMU to use only wind data from the towers in the cool season climatology. Stratification by stability was considered by the 45 WS but rejected due to a concern that it would not allow sufficient sample sizes to fit the parametric distributions being used for the peak speed ranges of operational concern. Temperature data from the towers or soundings were not QC'd since they were not required for this work. Merceret and Crawford (2010) found that tropical storm and non-tropical storm gust factors could not be compared properly without first stratifying the non-tropical storm data by stability. The non-tropical storm data were the same data used in this task. They confirmed the findings of previous studies (e.g. Monahan and Armendiraz 1971, Paulsen and Schroeder 2005) that stability is an important factor in the magnitude of peak winds. Peaks could tend to be higher in unstable conditions, and lower in stable conditions. Users of the GUI developed in this study must take this into account when interpreting the output values. Stratification by stability should be considered in future phases of this project.

3. Diagnostic Climatologies and Probabilities

The climatologies and probabilities described in the section are referred to as diagnostic to differentiate them from the prognostic probabilities discussed in Section 4. They are diagnostic because they reveal the characteristics of the peak speeds observed during the same 5-min period as their associated mean speeds. The prognostic probabilities show peak speed behavior in a set time period past the 5-min mean observation.

These values were calculated with the same methods used in Phase I (Lambert 2002). The QC'd observations were imported into the S-PLUS® software package for processing, and the processed data were then imported into Excel for display and GUI development.

3.1 Climatologies

The AMU modified scripts from the Phase I task to calculate the same climatologies for the new period of record. Those climatologies include

- Hourly means (μ) and standard deviations (σ) of the 5-min mean and peak speeds,
- Directional μ and σ of the 5-min mean and peak speeds in 10-degree bins, and
- Hourly/Directional μ and σ of the 5-min mean and peak speeds, stratified by direction in 45-degree bins.

3.1.1 Hourly Climatology

This product shows users the preferred times of day for higher 5-min mean and peak wind speeds. The hourly μ and σ of the 5-min mean and peak winds were calculated for each month and tower/height combination. The values were calculated using the 12 5-min winds in each hour for all days of each month and all years in the POR. Figure 3 shows an example of the hourly peak and mean speed climatologies for the 60-ft sensor on Tower 0393 at SLC 39A in February. The total number of possible observations in February was 104,832 (*12 obs/hr x 24 hrs/day x 28 days/Feb x 13 Febs*); and the total number of possible observations per hour was 4368 (*104,832 obs / 24 hrs*). The actual number of observations used to calculate the values was slightly lower due to missing and QC'd data, but was a sufficiently large sample from which to calculate reliable climatologies.
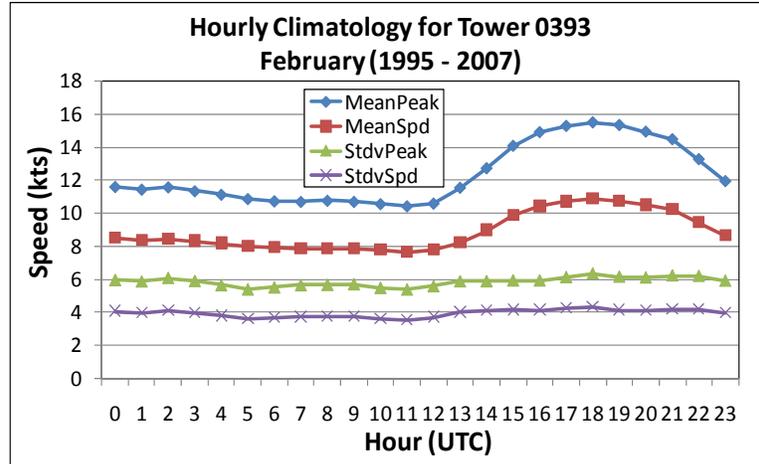
Figure 3. The hourly climatology for February at Tower 0393. The legend shows the curve colors for the μ of the 5-min peak (MeanPeak) and mean speeds (MeanSpd), and σ of the peak (StdvPeak) and mean speeds (StdvSpd).

The main feature seen in Figure 3 is the diurnal trend of μ in the peak and mean winds. This trend was evident in all the sensors. The local sunrise in February is between 1145 – 1215 UTC (0645 – 0715 EST), and sunset is between 2300 – 2330 UTC (1800 – 1830 EST). The mean speeds increased after sunrise and began decreasing several hours before sunset continuing through sunrise. The decrease after sunset was much more gradual than before sunset. The increase was likely caused by mixing down of higher momentum winds aloft by the convective updrafts and downdrafts created by daytime heating. The decrease may have been due to the reduction in surface heating and convective currents during the afternoon, and a nocturnal inversion that formed and continued to

13

intensify slowly after sunset and through the nighttime hours. Also noteworthy was the close correlation of μ between the peak and mean speeds. This supports the use of gust factors (Merceret 2009) to make first-guess forecasts of peak winds. The σ curves showed a large variability of near 6 kts for the peak speeds and 4 kts for the mean speeds with no diurnal variation. Forecasters must be aware of this variability when using these values.

3.1.2 Directional Climatology

This climatology was calculated to show users the monthly pattern in direction for stronger or weaker winds and a preferred direction based on the number of observations in each direction sector. The μ and σ of the 5-min mean and peak winds were calculated for 10° bins. The directional mean and peak speed climatology for February at Tower 0393 is shown in Figure 4a. The strongest speeds were from 340-360° (NNW) with a second maximum from 160-180° (S). Each month showed different directions for speed maximums and minimums. Note the close correlation between the μ of the peak and mean wind speeds and the large σ values as found with the hourly climatologies (Figure 3).

The number of peak and mean wind speed observations used in the calculations for Figure 4a are shown in Figure 4b. This climatology can reveal the predominant wind direction(s) for each month. Along with the maximum in mean speeds from the NNW and S, there were also maximums in the number of observations from these sectors. The gradual increase in the number of observations from the 70-160° sectors was interrupted by an anomalous drop at 120-150° (SE). Since Tower 0393 is located NW of SLC 39A, the drop in the number of SE wind observations is likely caused by the obstruction of flow around the launch pad to the SE. The magnitude of μ also decreased from these directions. The same patterns can be seen in the NW sectors of the Tower 0394 data, which is SE of the pad. This result emphasizes the need for redundant sensors on opposite sides of a tower or launch complex for observations critical to launch decisions.
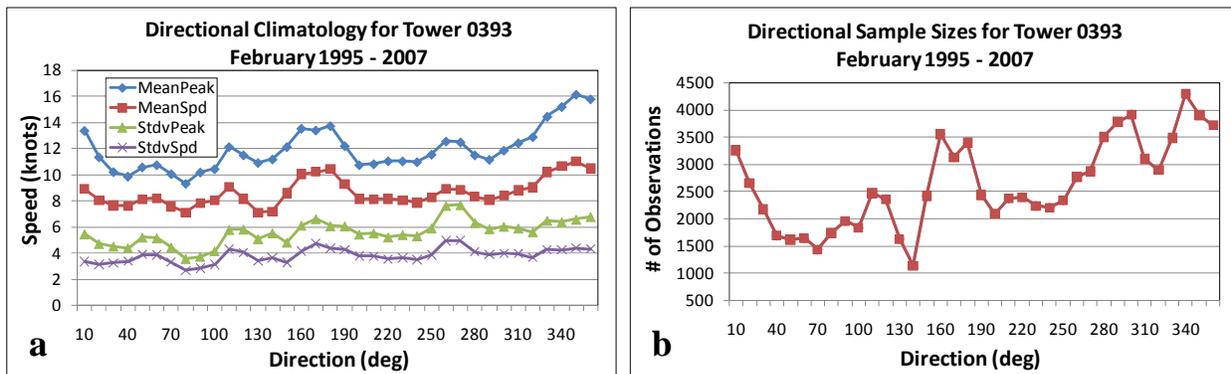

Figure 4. a) The same variables as in Figure 3, but for the directional climatology in 10° bins; and b) the number of observations in each 10° direction bin used to create the values in a.

3.1.3 Hourly/Directional Climatology

This climatology was calculated to show preferential times for stronger winds from specific direction sectors. The data were stratified by direction bin and then hour. The direction increments had to be small enough to derive meaningful wind direction climatologies, yet large enough such that a sufficient number of observations were available to calculate dependable values. Eight 45°-direction bins provided the best balance.

Figure 5 shows the hourly/directional climatology for the wind speeds from the 315-360° (NNW) direction bin. The highest peak speeds in the directional climatology (Figure 4a) were in this direction range. The highest peak speeds for the hourly (Figure 3) and directional climatologies (Figure 4a) were close to 16 kt at 1800 UTC (1300 EST) and 350°, respectively. The highest peak speed in Figure 5 is 19 kt at 1900 UTC (1400 EST), higher than in the other two climatologies. This product can show more precise climatological values for times and directions of interest than the separate hourly and directional climatologies. The values in Figure 3 and Figure 4 can be used to help the user focus on a particular hour/direction bin. The number of observations used to calculate the values in Figure 5a are shown in Figure 5b. There is a peak at 1500-1700 UTC (1000-1200 EST), showing that winds from the NNW were more likely to occur between local morning and noon in February.
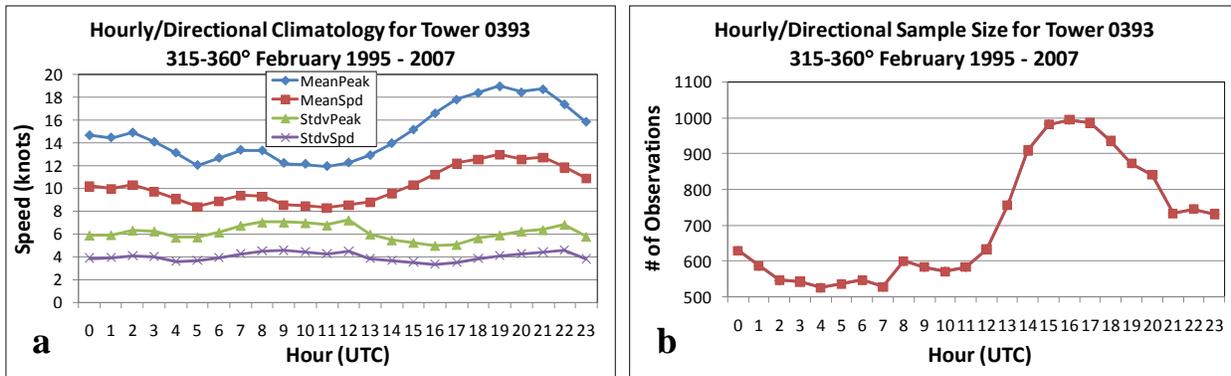
Figure 5. a) The same variables as in Figure 3, but for the hourly/directional climatology in the 315-360° (NNW) bin; and b) the number of observations in the 315-360° bin for each hour used to create the values in a.

3.2 Probabilities

As in Phase I, the AMU calculated the probability of meeting or exceeding a specific peak speed threshold given a 5-min mean speed. For every knot of mean wind speed, a range, or distribution, of peak speeds was observed over the 13-year POR. The distributions were used to create the empirical probabilities. The next step was to determine if a parametric distribution could be used to describe these empirical distributions. Finding such a distribution would serve a two-fold purpose: 1) to smooth over variations in empirical distributions, and 2) estimate probabilities of peak speeds beyond the range of the observations in the POR.

3.2.1 Empirical Distributions

To develop these distributions, the AMU stratified the peak winds by 5-min mean wind speed in 1-kt intervals and created empirical probability density functions (PDFs) of the peak winds for each month and sensor on each tower at each height. The PDF was calculated by dividing the number of observations of each individual peak speed in the distribution by the total number of observations associated with the mean wind speed. This produced a value representing the frequency of occurrence of each peak speed in the distribution. The sum of the frequencies in a PDF is, therefore, 1. Figure 6 shows the PDFs for Tower 0393 in February. Only the even mean speed PDFs in the range 6 – 30 kt are shown to keep the chart uncluttered and easy to interpret. Each curve represents a mean speed and each point on the curves represents the frequency of occurrence of the peak speed on the horizontal axis.
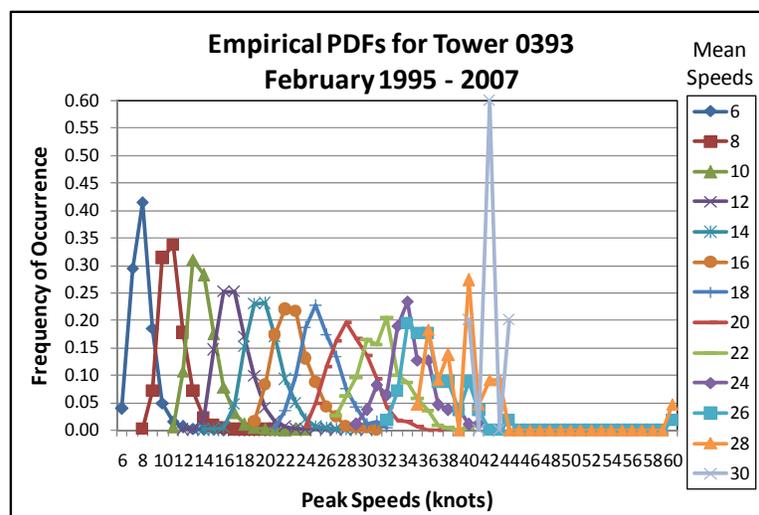

Figure 6. The empirical PDF curves for Tower 0393 in February. Each curve represents a mean speed whose symbol and color are shown in the legend at right. The vertical axis shows the frequency of occurrence of each peak speed in each PDF.

15

A cumulative distribution function (CDF) was created by integrating the PDF values from the lowest to highest peak speeds in the distribution. The CDF specifies the probability that a peak speed will not exceed a certain value (Wilks 2006). The 45 WS forecasters need to know the opposite: the probability of the peak speed meeting or exceeding a specific LCC value. To create the desired values, the AMU calculated complementary CDFs (C-CDFs), given by 1 – CDF. The peak speed C-CDFs derived from the PDFs in Figure 6 are shown in Figure 7a. Each symbol on a mean speed curve corresponds to a peak speed on the horizontal axis and a probability of meeting or exceeding that peak speed on the vertical axis. Note that the curves for mean speeds > 20 kt in Figure 6 and Figure 7a are not as smooth as those of the lower speeds. Figure 7b shows the total number of observations in each C-CDF. The value falls quickly from 957 at 18 kt to 393 at 20 kt, and then drops to 5 at 30 kt. The under-sampling of the 30-kt mean and associated peak speeds in the distribution resulted in an irregular curve in both Figure 6 and Figure 7a. The anomalous spike at 42 kt was due to three observations out of five having that peak speed. This shows that a small number of observations can create erroneous probabilities and be misleading to a forecaster.
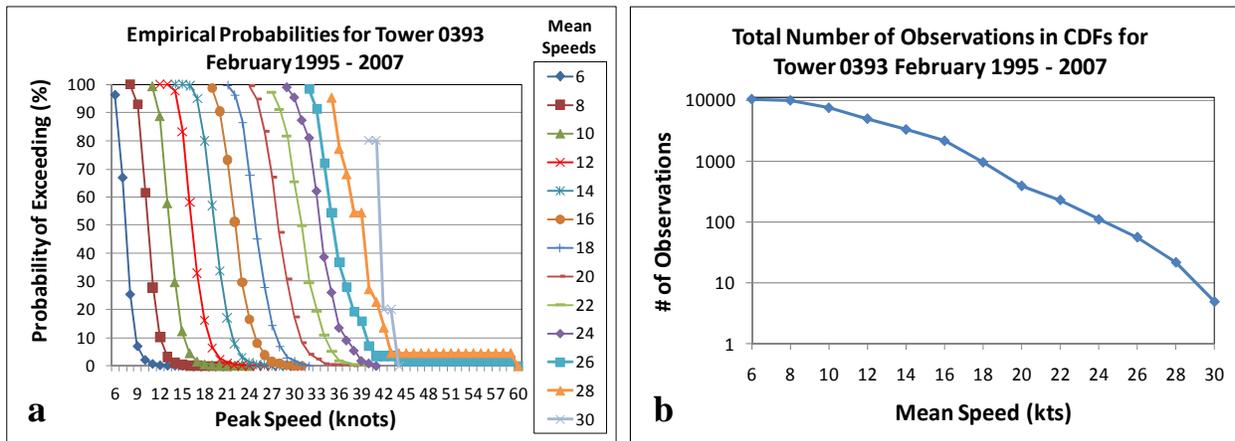

Figure 7. a)The C-CDF curves for Tower 0393 in February, and b) the number of observations of each mean speed used in creating the curves in a. Each curve in 7a represents a mean speed whose symbol and color are shown in the legend at right. The vertical axis in 7a is the probability of exceeding a peak speed in percent, and the vertical axis in 7b is logarithmic.

3.2.2 Parametric Distributions

As stated earlier in this report, there are two reasons for fitting parametric distributions to empirical distributions as defined in Wilks (2006). The first is to smooth over the variations in empirical distributions due to possible under-sampling of a specific peak gust. The second is to estimate probabilities of peak gusts associated with mean wind speeds outside the range of the observations in the data sample. The assumption inherent in the second reason is that the parametric distribution would also represent the peak wind distributions for rarely or as-yet unobserved mean wind speeds. Determining the validity of this assumption was difficult for the data in this study due to very small or non-existent sample sizes for such speeds. .

3.2.2.1 Gumbel Distribution Calculation

Fitting the C-CDFs with the proper parametric distribution was necessary for calculating the appropriate probability values, especially for extreme values that were observed only occasionally. In Phase I, the AMU used the Weibull distribution for this purpose since it had wide support in the literature to fit peak winds. However, the 45 WS requested the Gumbel distribution be used as the parametric distribution in the task since it has been proven to be the best fit for winds from the KSC/CCAFS wind tower network in studies conducted at MSFC. The Weibull and Gumbel are both extreme value distributions and share some similarities. Wilks (2006) identifies the Gumbel as an often-used extreme value distribution and, as such, is appropriate for peak winds. Using the Gumbel distribution would also make this work compatible with work done by the scientists at MSFC.

The Gumbel CDF is defined by the following equation in Wilks (2006):

$$F(x) = \exp\left\{-\exp\left[-\frac{x-\theta}{\beta}\right]\right\},$$

16

where x is the observed peak speed, θ is the location parameter related to the mean of the data sample, and β is the scale parameter related to the variance. The AMU used a two-step process to calculate the location and scale parameter values. The method of moments defined in Wilks (2006) was used to calcuate first-guess estimates of the parameters using the equations

$$\hat{\beta} = \frac{s\sqrt{6}}{\pi} \text{ and } \hat{\theta} = \bar{x} - \gamma\hat{\beta},$$

where s is the standard deviation of the peaks, $\bar{x}$ is the mean of the peaks, and γ is Euler's Constant (0.57721…). The first estimate values are usually not optimal, so the AMU employed the Chi-squared (X^2) goodness-of-fit equation to find the optimal values by iterating X^2 until it is minimized:

$$X^2 = \sum \frac{(\#Observed - \#Expected)^2}{\#Expected},$$

where *#Observed* is the number of observations for a peak value, and *#Expected* is the number of total observations in the distribution multiplied by the probability of the peak value. When the parametric distribution is fitted perfectly to the empirical, $X^2 = 0$.

In initial tests with the script, X^2 values indicated that the Gumbel distribution produced a good fit to the empirical C-CDFs. However, since the X^2 test was used to determine the distribution parameters, the AMU used another test, the Kolmogorov-Smirnov (K-S), to determine how well the computed parametric distributions fit the empirical distributions. The test statistic for the K-S test is

$$D_n = \max |F_n(x) - F(x)|,$$

where x is a peak speed along the CDF curve, $F_n(x)$ is the empirical probability of x, $F(x)$ is the parametric probability of x, and D_n is the largest absolute value difference between the empirical and parametric values in the distribution (Wilks 2006). If this number was sufficiently large, the null hypothesis that the sample was drawn from a population with a Gumbel distribution could be rejected. In each case, D_n was sufficiently small that the null hypothesis of these data coming from a Gumbel distribution could not be rejected at any level.

3.2.2.2   C-CDF Limit

Lambert (2002) found that the Weibull distribution could not be fit to empirical distributions created from 600 observations or less. Graphs of Weibull parameter values (mu, scale, and shape) versus mean speeds showed smooth curves for the range of lower mean speeds with > 600 observations, but became erratic at higher speeds with samples of ≤ 600. Unfortunately, it is the higher mean speeds that are more operationally significant. Therefore, in an attempt to model the Weibull parameters so that parametric C-CDFs for the higher speeds could be created, Lambert (2002) used best-fit polynomial regression equations to estimate the parameters beyond where the curves became erratic. The modeled and empirical values of the Weibull parameters for Tower 0397 in January from Lambert (2002) are shown in Figure 8. The modeled and empirical trends and values were similar for speeds up to 18 kt, but began to deviate at 19 kt, where the number of observations fell below 600. This was a consistent feature for other towers and months.

Lambert (2002) conducted tests to determine the validity of the two assumptions in modeling the Weibull parameters: 1) the distributions for the higher mean speeds were Weibull, and 2) their parameters followed a polynomial trend with mean speed. None of the test results supported these assumptions. It was possible that the Weibull parameters for the peak wind distributions of the higher mean speeds followed a different trend than those for the lower mean speeds. It was also possible that the phenomena that create higher mean and peak wind speeds resulted in different peak wind distributions than Weibull. The final conclusion from the tests was that the modeled parameters for the higher speeds could not be used with confidence, and only the speeds with > 600 observations would be estimated with the Weibull distribution.
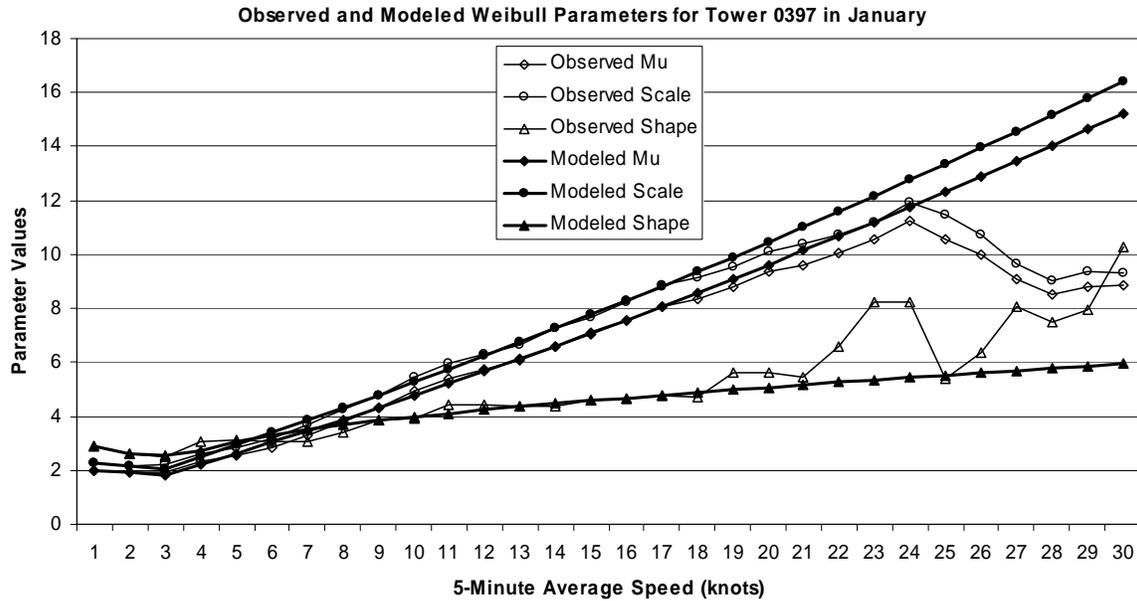
17

Figure 8. The empirical (thin lines) and modeled (thick lines) Weibull scale, mu, and shape parameter values for the peak wind speed PDFs based on the January 5-min mean wind speeds from 1 - 30 kts at Tower 0397 [Figure 11 from Lambert (2002)].

As with the Weibull distributions in Lambert (2002), the Gumbel distributions could not be fit to higher mean speed distributions with fewer observations. To determine the appropriate threshold criteria for mean speed distributions that could not be estimated, the AMU examined the Gumbel location (θ) and scale (β) parameters along with the number of observations in each distribution. The observation number threshold varied between 400 and 100. Since the number of observations at the cutoff point varied, other criteria were needed. Further analysis of the Gumbel parameters found the changes in θ and β between consecutive mean speeds defined the cutoff mean speed distribution well. The final algorithm isolated the mean speed distributions with ≥ 100 and ≤ 400 observations, then chose lowest speed with the highest change in θ or β from the previous speed as the cutoff. Gumbel distributions were calculated for all speeds less than the cutoff speed.

Figure 9 demonstrates how this method was used. For the 54 ft sensor on Tower 0020 in December, there were 428 observations of 16-kt mean winds, 224 17-kt mean winds, 122 18-kt mean winds, and 69 19-kt mean winds. This put 17 and 18 kt within the 100 – 400 observation range, indicated by the black vertical lines. The largest change in θ and β in this range occurred at 18 kt, highlighted by the red ellipse, suggesting this is where the Gumbel distributions become unstable and should not be used for mean speeds ≥ 18 kt. Therefore, Gumbel distributions were calculated for all mean speeds ≤ 17 kt. Above 18 kt, the slopes of the parameter curves become erratic. This is likely due to the small number of observations for these higher speeds. In Lambert (2002), the highest speed modeled for this tower/height/month stratification was 14 kt. The combination of more observations due to a longer period of record and the ability of the Gumbel formulation to model empirical distributions with < 600 observations allowed higher speeds to be modeled at every tower and height.
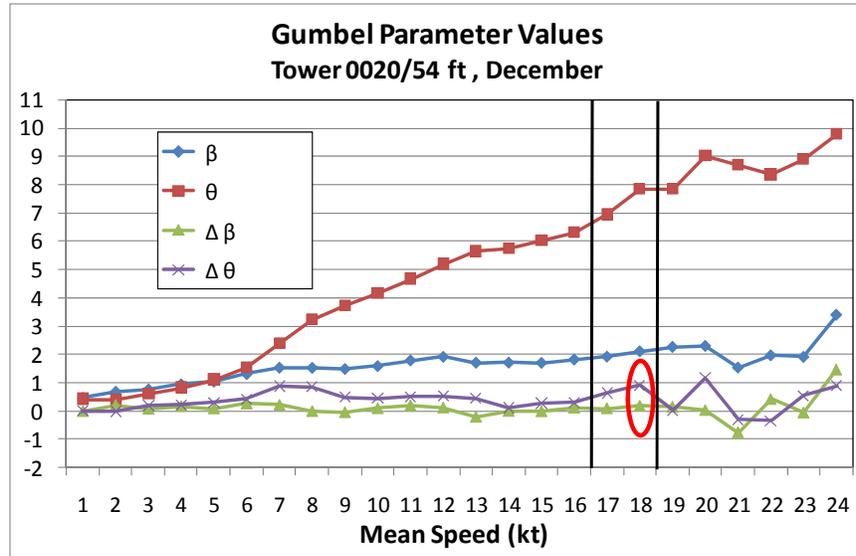
18

Figure 9. The Gumbel parameters, θ and β, for each mean wind speed and their change in value ($\Delta\theta$ and $\Delta\beta$) from the previous mean wind speed. The mean speeds (kt) are on the x-axis and the parameter values (dimensionless) are on the y-axis. The black vertical lines outline the range of mean speeds with 100 – 400 observations, and the red ellipse outlines the largest $\Delta\theta$ and $\Delta\beta$ within the vertical lines.

4. Prognostic Probabilities

The prognostic probabilities provide the probability of meeting or exceeding a specified peak speed within a specified time period after a 5-min mean speed observation. The time periods requested by the 45 WS were 2, 4, 8, and 12 hours and they requested the probabilities be stratified by hour. They also requested that the distributions be fit with a parametric distribution as was done for the diagnostic probabilities (Section 3.2.2)

4.1 Data Processing

The AMU developed a re-sampling technique to process and prepare the data for calculating the empirical prognostic probabilities that used all 5-min mean and peak speeds in the data set. Figure 10 demonstrates how the data were collected for the 2-hour time interval after 0000 UTC. The 12 mean speeds in the 30 min intervals before and after the central time of 0000 UTC represent the mean speeds for that hour. This time period, 2330–0025 UTC, is highlighted in blue in Figure 10. The brackets above the timeline encompass the range of times from which the peaks are drawn for the first and last times in the blue area. The peak speeds associated with the mean speed at 2330 UTC were taken from the time period 2335 - 0125 UTC. The peaks associated with the mean speed at 0025 UTC were taken from the time period 0030 - 0220 UTC. This technique assured that every mean speed in the data set was used, but also meant that the same peak speed would be used, or re-sampled, in multiple distributions.

The same procedure was followed for every 5-min mean speed between 2330 and 0025 UTC and for every 0000 UTC in each month. For the 2-hour prognostic probabilities, this resulted in 23 peak speeds associated with each mean speed at the times surrounding 0000 UTC. Each set of 23 peak values was binned with its associated mean speed. This was done for each hour of every day in each cool-season month and for each individual tower/height combination. The same procedure was followed for the 4-, 8-, and 12-hour probabilities, resulting in 47, 95, and 143 peak speeds per set, respectively.
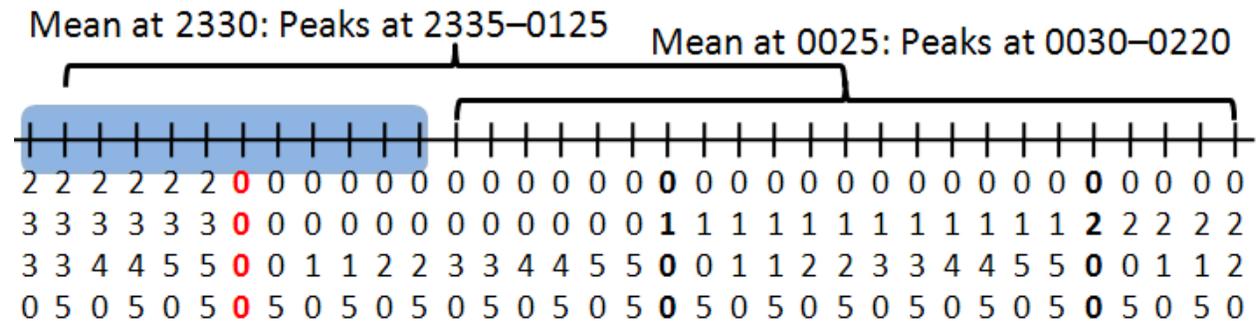

Figure 10. Timeline demonstrating how the data for the 2-hour probabilities at 0000 UTC were collected. The times highlighted in blue represent the set of 5-min mean speeds. The brackets above the timeline represent the range of times over which the 5-min peaks were collected for the first and last mean speed observations in the blue shaded area. The time of interest, 0000 UTC, is highlighted in red.

The 2-hour sets, identified by a mean speed and 23 peak speeds, were combined with sets having the same mean speed. This reduced the number of sets to the number of different mean speeds in each hour. For example, the first step in the procedure would create 360 1-mean/23-peak sets for a specific hour in a month with 30 days. The sets with identical mean speeds were combined. If there were 20 different mean speeds in the set of 360, the end result would be 20 sets with a large number of peak speeds in each. These distributions were used to calculate the empirical C-CDFs for each hour/month/tower/height. Each mean speed then had a distribution of peak speeds associated with it.

4.2 Empirical Prognostic C-CDFs

The empirical 2-hour prognostic probabilities for Tower 0020/54 ft at 0400 UTC are shown in Figure 11. These are interpreted as the probability of meeting or exceeding a specific peak speed over the next two hours (04–0600 UTC) given the empirical 5-min mean speed at 0400 UTC. The C-CDF curves for mean speeds higher than 12 kt were not smooth, but erratic, and some curves began crossing each other at 13 kt (red curve) and higher. Increasing the observations for each hour through the re-sampling technique did not help define the C-CDFs for the higher and more operationally critical speeds. This created difficulty in determining the appropriate parametric distribution for modeled C-CDFs, even for lower speeds.
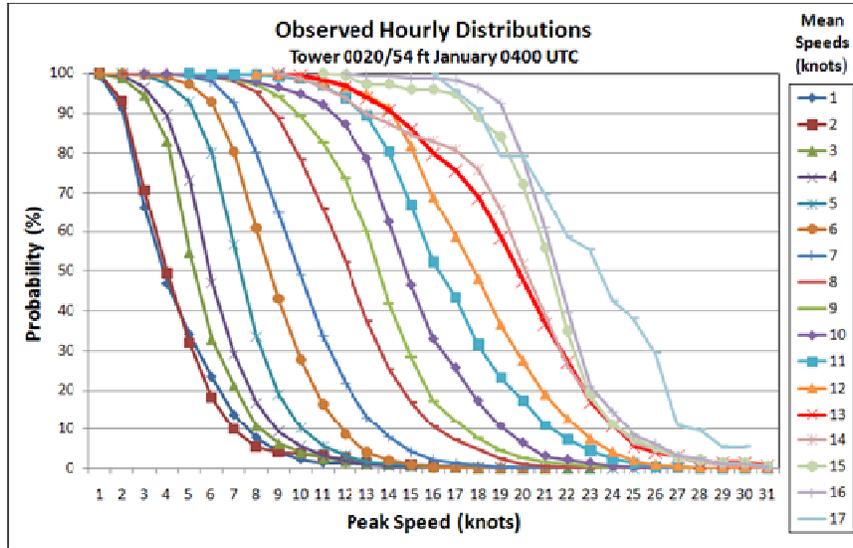
Figure 11. The empirical 2-hour prognostic C-CDFs from Tower 0020/54 ft at 0400 UTC in January. The legend shows the colors associated with each 5-min mean speed curve.

After reviewing the 2-hour prognostic data for each hour at several towers, the AMU concluded that there were not enough data to stratify by hour and properly model the higher wind speeds important to operations. Therefore, the AMU combined the hourly values into 3-, 6-, 12- and 24-hour (i.e. no time stratification) groups in an attempt to alleviate the two issues described in the previous paragraph. The 3-, 6-, and 12-hour groupings (not shown) exhibited similar issues to the 1-hour data. Eliminating the time stratification resulted in smooth curves more conducive to determining an appropriate parametric fit. The empirical 2-hour prognostic probabilities for Tower 0020/54 ft with no time stratification are shown in Figure 12. The AMU combined the hourly files into one for each month/tower/height combination and created the non-time-stratified empirical probabilities.
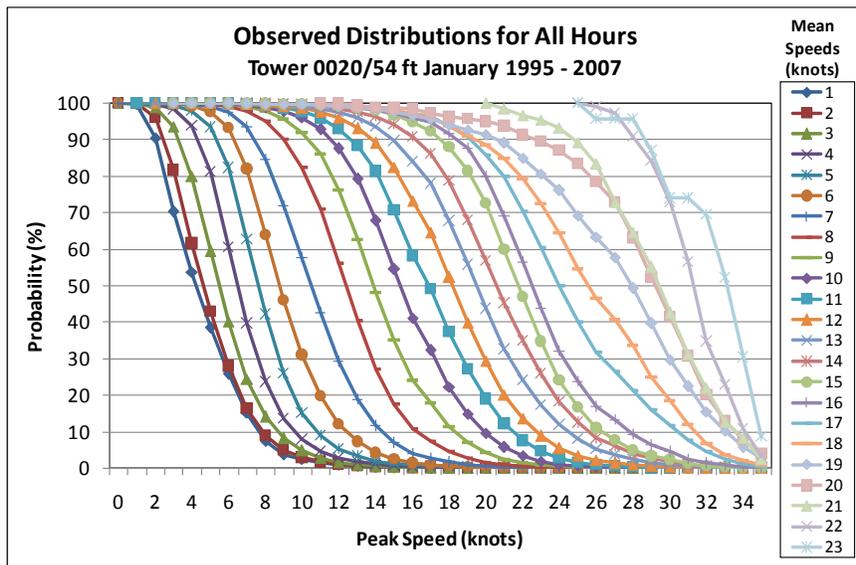

Figure 12. Same as Figure 11, but for no time stratification.

4.3 Parametric Prognostic C-CDFs

Using the procedure described in Section 3.2.2, the AMU calculated the Gumbel parameters for the 2-hour probabilities in Figure 12 and other month/tower/height combinations. The Gumbel distribution did not fit the data in any case. Two other well-known extreme value distributions, the Weibull and Generalized Extreme Value (GEV) distributions (Wilks 2006) were tested, as well as the Gaussian distribution. None of these distributions fit the data.

Figure 13 shows an example of the parametric distributions created using the data in Figure 12. The black curve is the empirical C-CDF of the 2-hour probabilities for the 15 kt 5-min mean speed (in Figure 12, green curve with solid circle marker). In the range 15–22 kt peak speed, the Gumbel distribution estimated probabilities too low, and from > 23 kt it estimated probabilities too high. The Weibull distribution estimated probabilities too high from 17–31 kt peak speeds. The Gaussian and GEV distributions provided the best fit, but still overestimated the probabilities between 21 and 31 kt peak speeds. Between 25 and 31 kt peak speeds, the GEV distribution overestimated the probabilities more than the Gaussian.
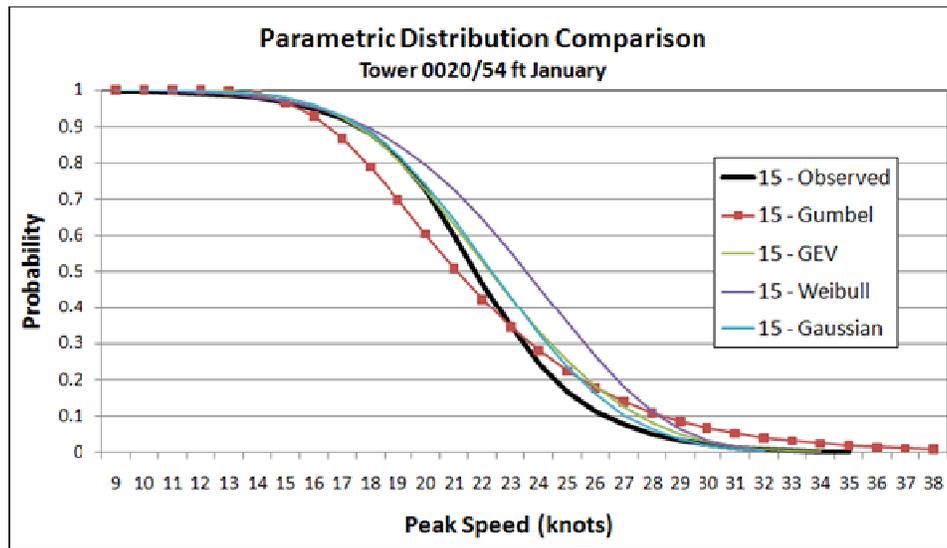

Figure 13. The empirical and modeled C-CDFs from Tower 0020/54 ft in January for the 15 kt 5-min mean speed. The legend at right shows the curve colors associated with each model and the observations. The empirical C-CDF is solid black.

After examining several charts similar to Figure 13 and consulting with the KSC Weather Office and 45 WS, the AMU concluded that no single parametric distribution could be used to model the prognostic probabilities. While the Gumbel distribution provided an excellent fit to the diagnostic probabilities, it did not in this case. One reason could stem from combining data over several hours using a re-sampling technique. Different physical mechanisms could be dominant at different times. There may or may not be a parametric distribution that can fit these data. If there is, it may be a combination of the above-mentioned distributions. It would be difficult to determine the percent contribution of each. Due to these issues, only the empirical 2-, 4-, 8-, and 12-hour prognostic probabilities will be available in the GUI.

These values, as well as those described in Section 3, will not be used to make absolute probability forecasts of peak winds. The forecasters will use observations, model data, and their experience and knowledge of peak wind behavior in the KSC/CCAFS area to determine the final probability value.

5.   Graphical User Interface

The forecasters requested that a PC-based GUI be developed to display the requested information quickly and in an easy-to-interpret format. A similar GUI was developed in Phase II (Lambert 2003) using VBA in Excel 2003. The GUI developed for Phase III was based on the Phase II GUI but modified using Excel 2007 to contain features needed by the 45 WS forecasters.

In Phase I, all of the climatologies and probabilities were provided in Excel Pivot Charts. These charts are very flexible, allowing changes with point-click-drag techniques. Axes can be switched, multiple variables can be represented on one axis, and specific curves can be temporarily removed from the display to facilitate closer examination of other curves. However, confident use of the Pivot Charts required training and experience and were difficult to manipulate and interpret in the operational environment. The final GUI described in this section resulted from several consultations between the AMU and 45 WS. They were shown the GUI at several steps in the development to test and make suggestions for modifications, all of which were incorporated. This ensured that the end product met their needs, was easy to use, and produced useful information in a readable format.

This GUI was delivered to the 45 WS in stages as each climatology and probability was created and incorporated. The AMU included a memorandum with the first distribution of the GUI to describe how to interact with Excel 2007 and how to use the interim version of the GUI (Crawford 2009). The information in Sections 5.1 – 5.3 of this report supersede the information in Section 2.3 of the memorandum. All other sections in the memorandum describing how to interact with Excel 2007 are valid.

5.1   Initial Form

The GUI starts automatically when opening the file LCC.PK.WIND.GUI.xlsm. The initial form has two tabs, one for the climatologies and the other for the probabilities. Figure 14a shows the "Climatology" tab and Figure 14b shows the "Probability" tab. On both tabs, the user chooses the tower, sensor height, and month of interest. The tower must be chosen before the height because the choice of heights in the drop-down list is limited to the heights on the tower displayed in the "Tower" text box. The specifics of the other choices on each tab are discussed in Sections 5.2 and 5.3.
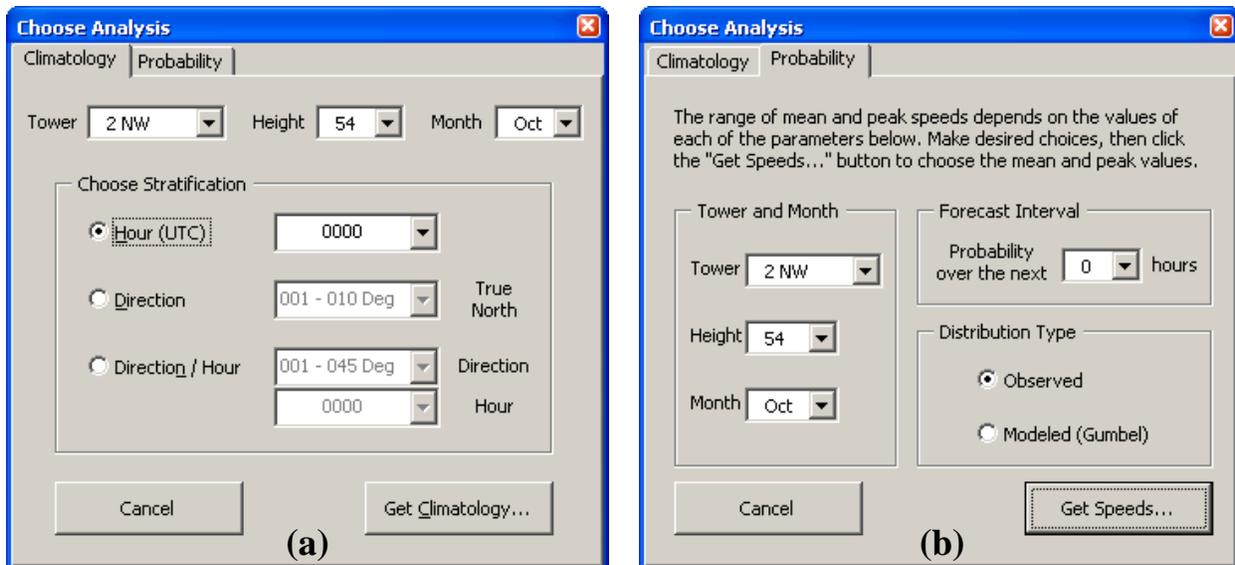

Figure 14.   The Climatology (a) and Probability (b) tabs in the initial GUI form.

5.2   Climatology

After choosing tower, height, and month on the "Climatology" tab, the next step is to choose one of the three stratifications and the desired hour and/or direction sector in the text boxes next to the name of the chosen stratification. After all choices are made, the user will click the "Get Climatology..." button and an output form with the retrieved information will be displayed. There are three output forms, one for each stratification on the "Climatology" tab. The three output forms have identical formats.

23

Figure 15 shows the "Climatology" tab (a) and the "Requested Climatology" output form for the hourly stratification (b). The "Tower" drop-down list is shown in Figure 15a with Tower 0393 chosen, where 39A-N means this tower is on the north side of SLC 39A (Figure 1). After choosing this tower, "Height" changes to 60 ft automatically. That is the only sensor height on this tower. For other towers with two heights, the choices will be in a drop-down list. The "Month" is November, and the "Hour" is the default 0000 UTC. The drop-down lists for "Direction" and "Direction/Hour" are de-activated and set to light gray to show which stratification was chosen.

The top portion of the output form in Figure 15b reiterates the information chosen in the "Climatology" tab (Figure 15a). The words "and Direction" and the text box to the right are grayed out to show this climatology was not chosen in the tab. The climatology values are displayed in the "Wind Statistics" section. This includes the average, standard deviation, and number of observations for the mean and peak wind speeds. Next to this section is the "Choose Another Analysis" button used to close the output form and return the user to the initial tab. The notice at the bottom reminds users that the values displayed were calculated from historical data, not currently observed data, and should not be used as an absolute forecast for future winds.
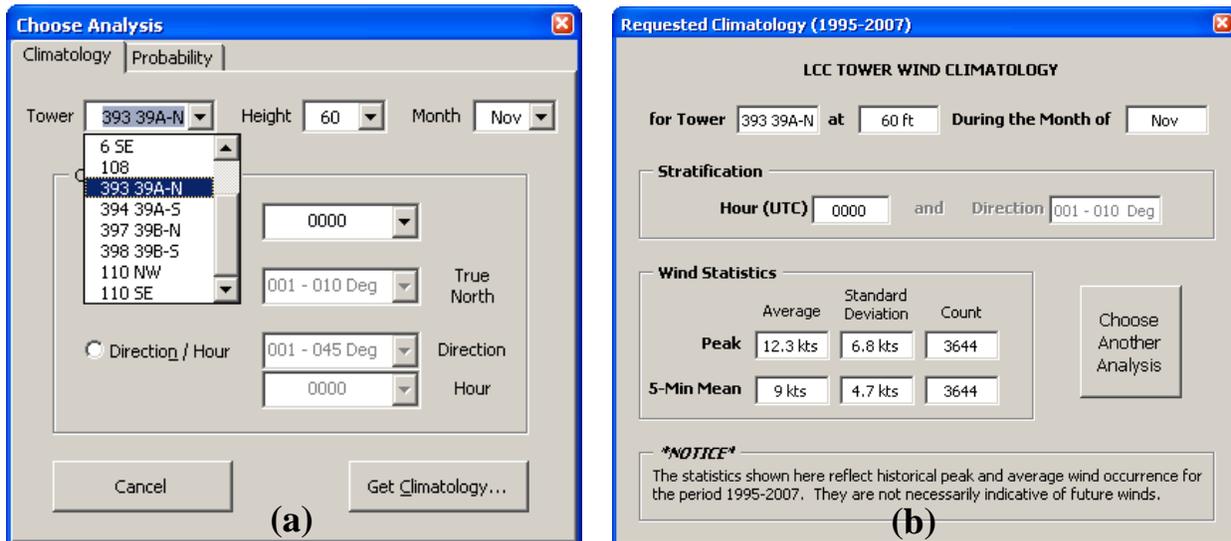

Figure 15.   a) The "Climatology" tab of the initial GUI with the height drop-down list displayed, and b) the "Requested Climatology" output form showing the hourly mean and peak wind speed climatology values for Tower 0393/60 ft at 0000 UTC in November.

Figure 16 shows the output forms for the "Direction" (a) and "Direction/Hour" stratifications. The type of information displayed at the top is the same as for the hourly climatology in Figure 15b. Below this, the user's choice of hour and/or direction bin is displayed. The text "Hour (UTC)" and the text box to the right are grayed out in Figure 16a to show that climatology was not chosen in the initial form. The "Wind Statistics" section for the directional climatology in Figure 16a includes the same statistics as for the hourly climatology. The same is true for the directional/hourly climatology in Figure 16b except that the number of observations is replaced by the percent of total observations in the hour. Since the number of observations from a particular direction sector can vary by hour, this value does not provide enough information about whether a certain direction was more or less common for a particular hour. If all observations in a particular hour were evenly divided between all eight sectors, the value in this box would be 12.5% for every sector. Values larger or smaller than this would show forecasters whether winds from a particular sector were more or less prevalent for a certain hour.
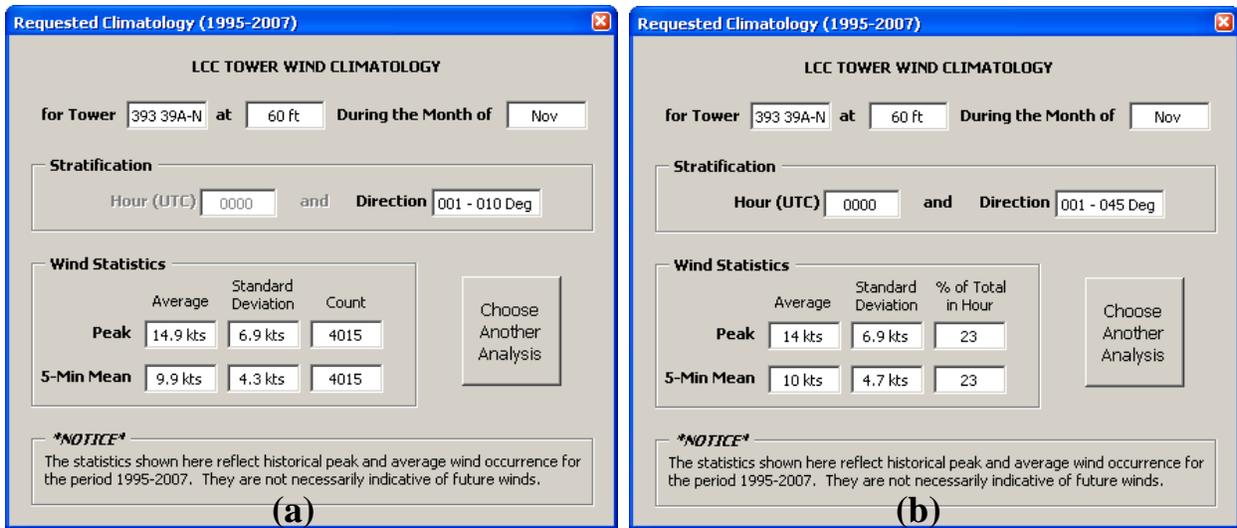
Figure 16. The "Requested Climatology" output forms showing the directional (a) and directional/hourly (b) mean and peak wind speed climatology for Tower 0393/60 ft at 0000 UTC in November

5.3 Probability

After choosing the tower, height and month on the "Probability" tab, the user will choose the "Forecast Interval" and "Distribution Type". The "Forecast Interval" choices are the diagnostic (0 hours) or prognostic (2, 4, 8, or 12 hours) probabilities. When 0 is chosen, the user can choose the observed diagnostic probabilities or those modeled with the Gumbel distribution, as described in Section 3.2. Figure 17a shows the "Probability" tab with 0 hours for the "Forecast Interval". "Observed" and "Modeled (Gumbel)" are active in the "Distribution Type" section, meaning either can be chosen. Figure 17b shows the "Forecast Interval" drop-down list with the 8-hour prognostic time period chosen. Note that "Modeled (Gumbel)" in the "Distribution Type" section is grayed out, indicating that it cannot be chosen. Recall from Section 4.3 that the prognostic probabilities were not modeled with a parametric distribution and only the observed probabilities would be available in the GUI.
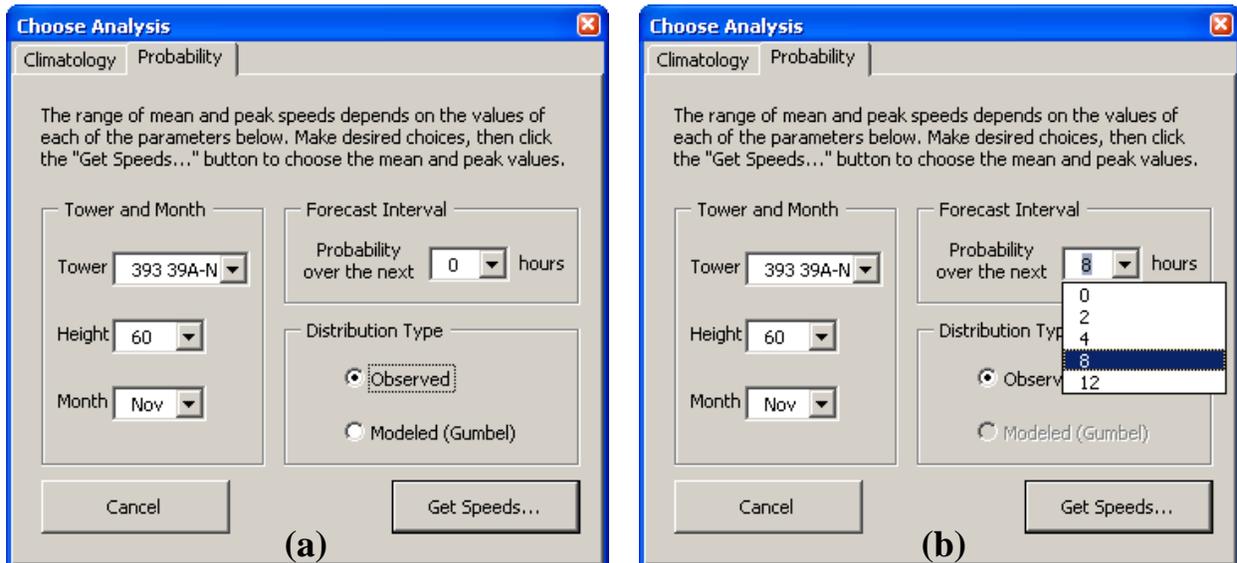

Figure 17. The initial Probability tab showing the choices for the diagnostic (a) and prognostic (b) probabilities.

25

Once all choices are made in the "Probability" tab, the user clicks the "Get Speeds..." button and the "Choose Mean and Peak" form in Figure 18 appears. It allows the user to choose the mean and peak speeds of interest. The choices in the initial form (Figure 17) determine the range of mean speeds in the drop-down list, and the choice of mean speed determines the range of peak speeds. Figure 18 shows the form after 15 kt and 23 kt were chosen as the mean and peak, respectively, from drop-down lists. The "New Parameter Values" button takes the user back to the "Probability" tab to change the input parameters if desired. Clicking the "Get Probability…" button displays the output form with the desired probability values.
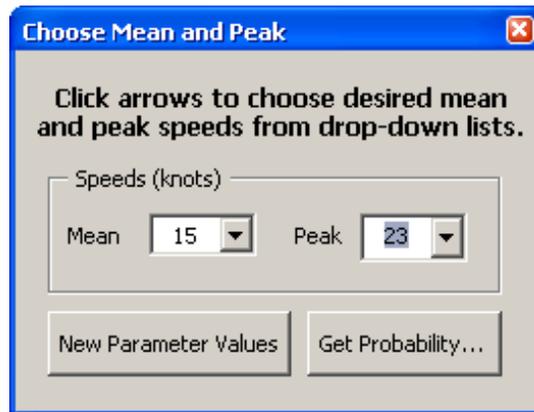

Figure 18.   The form to choose the mean and peak speed of interest, displayed after clicking "Get Speeds..." in the Probability tab (Figure 17a).

Figure 19a shows the "Choose Mean and Peak" form output when a prognostic value for "Forecast Interval" in Figure 17b is chosen. For the diagnostic probabilities, it is not possible to have a peak speed lower than the mean since the peaks are from the same 5-min period as the mean. However, it is possible to have lower peak speeds over a time period after a mean is observed, in this case within 8 hours after the mean. The top portion of the peak speed drop-down list in the "Choose Mean and Peak" form is shown to demonstrate this. In Figure 19a, 10 kt was chosen for the peak speed. This is less than the chosen mean speed of 15 kt. When this happens, the "Peak Wind Value Warning" form in Figure 19b is displayed when the "Get Probability..." button is clicked in Figure 19a. It lets the user know that a peak speed less than the mean was chosen and provides the choice of proceeding or not. Clicking the "No" button will close the warning form and return the user to the "Choose Mean and Peak" form where a new peak value can be chosen.
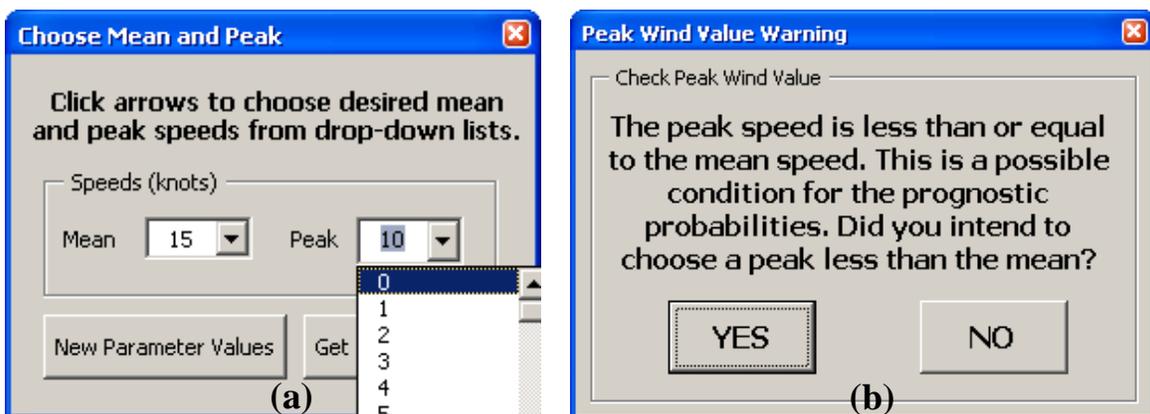

Figure 19. a) The "Choose Mean and Peak" form displayed when the Forecast Interval is set to one of the prognostic probability periods, in this case 8 hours (Figure 17b); and b) the warning form displayed when the peak speed chosen is less than the mean speed.

26

When "Get Probability..." in the "Choose Mean and Peak" form or "Yes" in the warning form is clicked, the "Requested Probability" output form is displayed. User-input from the first two forms is repeated at the top, and the probability is displayed in large font. Figure 20 shows the results from the choices in Figure 17a and Figure 18. The notice at the bottom left is similar to the statement on the climatology output forms. It reminds users that the values displayed were calculated from historical data, not currently observed data, and should not be used as an absolute forecast for future winds. The "Retrieve Another Peak Speed Probability" button closes the form and returns the user to the "Choose Mean and Peak" form.

Figure 20. Output form displayed for the diagnostic and prognostic probabilities after clicking the "Get Probability..." button in the mean and peak choice form.

6.   Summary

Accurate forecasts of peak winds are critical to protecting the safety of launch pad workers on KSC/CCAFS and preventing financial losses due to delays and damage. However, forecasters indicate that peak winds are a challenging parameter to forecast, particularly in the cool season. To help alleviate the difficulty in forecasting peak winds, the 45 WS tasked the AMU to

- Update the Phase I peak speed statistics for the LCC towers by increasing the POR from 7 to 13 years,
- Test the Gumbel distribution to model the peak speed probabilities,
- Create prognostic probabilities of peak winds within 2, 4, 8, and 12 hours of a mean speed observation, and
- Develop a GUI to display the desired values.

The AMU met all goals in this work and delivered the GUI to the 45 WS for operational use.

While stability is an important factor in the magnitude of peak winds, the data were not stratified by stability due to customer requirements. Users of the GUI must take this into account when interpreting the output.

6.1   Statistics

The AMU created the climatologies of the mean and peak wind speeds similar to those in Phase I using the three stratifications of hour, direction, and direction/hour for each tower, height, and month. It is important to note that the climatologies are smoothed values of highly variable data and are not to be used to determine the mean and peak winds for a particular time on a particular day. These values would be useful in the time leading up to an operation to show forecasters the average speeds at a particular tower and height for a particular month, hour, and/or direction. In particular, the direction/hour climatology shows the climatologically preferred direction sector for each hour in the day as well as the average mean and peak speeds.

After the climatologies, the AMU created the diagnostic peak speed probabilities for the 5-min mean speeds in 1-kt intervals. Diagnostic indicates that the peak speeds were associated with the mean speed from the same 5-min period. Tests revealed that the Gumbel distribution was a good fit to the data, except for the higher speeds. The AMU developed an objective two-step algorithm to determine the highest speed that could be modeled with the Gumbel distribution. The first step narrowed the distributions to those with < 400 but > 100 observations. The second step calculated the change in the Gumbel parameters between the distributions within the 400-100 observation range. The cutoff was the distribution with the largest change in one or both of the Gumbel parameters. In Phase I, wind speeds with < 600 observations could not be modeled with the Weibull distribution. More data due to a longer POR and the new objective cutoff method allowed higher speeds with fewer than 600 observations to be modeled in this phase.

The final set of statistics calculated were the prognostic probabilities that provide the probability of meeting or exceeding a specified peak speed within a specified time period after a 5-min mean speed observation. The time periods requested by the 45 WS were 2, 4, 8, and 12 hours. They also requested that the peak probabilities be fit with a parametric distribution as was done for the diagnostic values. The AMU developed a re-sampling technique that used all 5-min mean and peak speeds in the data set in preparing the data to calculate the empirical probabilities. However, results from several tests showed that no single parametric distribution could be used to model the prognostic probabilities. Therefore, only the empirical 2-, 4-, 8-, and 12-hour prognostic probabilities were calculated.

All climatology and probability values calculated in this task represent historical wind behavior. They are not predictive, and should not be used as an absolute forecast of future winds. They are intended to assist in making the forecast as an objective first guess. Model output, current observations, and forecaster experience should be used along with this tool to make a confident peak wind forecast.

6.2   Operational GUI

The 45 WS also requested a PC-based GUI to display the probabilities and climatologies quickly and in an easy-to-interpret format. The AMU modified the GUI developed in Phase II (Lambert 2003) to contain features needed by the 45 WS forecasters. The climatology and probability values for all the towers are contained in one Excel file.

In Phase I, the tool delivered to the 45 WS was a set of Excel files containing Pivot Charts of the climatologies and probabilities. These displays were very flexible, allowing changes to the charts with point-click-drag techniques. However, the Pivot Charts were difficult to manipulate and interpret in the operational environment. After seeing the success of the GUI developed in Phase II for SMG, the 45 WS forecasters requested a similar tool. The GUI described in Section 5 is the result of several consultations between the AMU and 45 WS. This ensured that GUI met their needs, was easy to use, and produced useful information in a readable format.

6.3   Future Work

Several factors create higher average wind speeds and influence the intensity of peak winds on KSC/CCAFS. The phenomena responsible for high mean and peak speeds include frontal passages, convective outflow boundaries, and the mixing down of high momentum air from aloft. The atmospheric stability in the boundary layer is also an important factor for gusts, as is the location of the wind sensor relative to the ocean (i.e. how far inland) and how much vegetation surrounds the site.

The peak speed distributions caused from any of these factors could result in different parametric distributions. In this study, the Gumbel distribution produced a good fit to the diagnostic C-CDFs created from distributions with at least 100 observations, but not the higher speeds with fewer observations. It is important to keep in mind that the factors creating gusts at higher speeds also create gusts at the well-sampled lower speeds. It is possible that the peak speed distributions at the lower mean speeds are the sum of a mixture of multiple population samples with different distributions. The different phenomena that cause gusts could be mixed together, and each could create their own distribution that is not necessarily Gumbel, but the sum of which is approximately Gumbel.

The best way to determine the proper distributions would be to create data stratifications based on meteorological phenomena and other physical properties such as topography around the tower and stability. Merceret and Crawford (2010) determined that any future work in comparing tropical storm gust factors to those from non-tropical storm environments will require the data to be stratified by stable, neutral, and unstable environments as stability is a critical factor in the occurrence and magnitude of peak winds. Stratifying the data by phenomena such as stability would have required time and resources beyond the scope of this task. Sounding or tower temperature data could be used to determine stability, but a complex algorithm would have to be developed to recognize the patterns and observations associated with other meteorological phenomena. Also, care must be taken not to stratify the data with too many categories to avoid creating samples too small to calculate robust statistics. One option to avoid this would be to not stratify by month or hour, but rather by the physical properties and phenomena that create peak winds. In any case, future work on this topic must include stratification by physical processes as opposed to calendar dates and/or clock time.

29

References

Crawford, W. C., 2009: Interim Graphical User Interface for LCC Tower Peak Wind Climatology. AMU Memorandum, January 2009, 9 pp. [Available from ENSCO, Inc., 1980 N. Atlantic Ave., Suite 830, Cocoa Beach, FL, 32931.]

Lambert, W. C., 2002: Statistical short-range guidance for peak wind speed forecasts on Kennedy Space Center/Cape Canaveral Air Force Station: Phase I Results. NASA Contractor Report CR-2002-211180, Kennedy Space Center, FL, 39 pp. [Available from ENSCO, Inc., 1980 N. Atlantic Ave., Suite 830, Cocoa Beach, FL, 32931 and online at http://science.ksc.nasa.gov/amu/final-stfi.html.]

Lambert, W. C., 2003: Extended Statistical Short-Range Guidance for Peak Wind Speed Analyses at the Shuttle Landing Facility: Phase II Results. NASA Contractor Report CR-2003-211188, Kennedy Space Center, FL, 27 pp. [Available from ENSCO, Inc., 1980 N. Atlantic Ave., Suite 830, Cocoa Beach, FL, 32931 and online at http://science.ksc.nasa.gov/amu/final-stfi.html.]

Monahan, H.H. and M. Armendariz (1971): Gust Factor Variations with Height and Atmospheric Stability, J. Geophys. Res., **76**, 5807 - 5818

Merceret, F. J., 2009: Two Empirical Models for Land-falling Hurricane Gust Factors, *National Weather Digest*, **33(1)**, 27-36.

Merceret, F. J. and W. C. Crawford, 2010: A Comparison of Tropical Storm (TS) and Non-TS Gust Factors for Assessing Peak Wind Probabilities at the Eastern Range. *14th Conference on Aviation, Range, and Aerospace Meteorology*, 5.6, Atlanta, GA, Amer. Meteor. Soc., 6 pp. [Available online at http://ams.confex.com/ams/90annual/techprogram/paper_156464.htm.]

Paulsen, B. M. and J. L. Schroeder, 2005: An Examination of Tropical and Extratropical Gust Factors and the Associated Wind Speed Histograms, J. Appl. Meteor., **44**, 270 -280.

Wilks, D. S., 2006: *Statistical Methods in the Atmospheric Sciences*. 2d ed. Academic Press, Inc., San Diego, CA, 467 pp.

List of Acronyms

45 WS	45th Weather Squadron	KSC	Kennedy Space Center
AMU	Applied Meteorology Unit	LCC	Launch Commit Criteria
CCAFS	Cape Canaveral Air Force Station	PDF	Probability Density Function
CDF	Cumulative Distribution Function	POR	Period of Record
C-CDF	Complementary CDF	QC	Quality Control
FR	Flight Rules	RH	Relative Humidity
GEV	Generalized Extreme Value	SMG	Spaceflight Meteorology Group
GUI	Graphical User Interface	VBA	Visual Basic for Applications (Excel)

NOTICE